

## Magnetization studies of phase separation in $\text{La}_{0.5}\text{Ca}_{0.5}\text{MnO}_3$

R. S. Freitas and L. Ghivelder\*

*Instituto de Física, Universidade Federal do Rio de Janeiro, C.P. 68528, Rio de Janeiro, RJ 21945-970, Brazil*

P. Levy and F. Parisi

*Departamento de Física, Comisión Nacional de Energía Atómica, Av. Gral Paz 1499 (1650) San Martín, Buenos Aires, Argentina*

(Received 17 September 2001; published 1 February 2002)

We present magnetization studies in a series of phase-separated  $\text{La}_{0.5}\text{Ca}_{0.5}\text{MnO}_3$  manganite samples, with different low-temperature fractions of the ferromagnetic (FM) and charge-ordered antiferromagnetic phases. A particular experimental procedure probes the effect of the magnetic field applied while cooling the samples, which promotes FM fraction enlargement and enhances the melting of the charge-ordered phase. The response of the system depending on its magnetic field history indicates the existence of three different regimes in the phase-separated state which develops below  $T_C$ . Our data allow us to identify the onset temperature below which the system becomes magnetic and structurally phase separated and an onset field above which FM fraction enlargement occurs.

DOI: 10.1103/PhysRevB.65.104403

PACS number(s): 75.30.Vn, 72.80.Ga, 75.30.Kz

### I. INTRODUCTION

The mixed-valent manganites  $R_{1-x}A_x\text{MnO}_3$  ( $R$ =rare earth,  $A$  = Ca, Sr, or Ba) have attracted considerable scientific interest due to their wide variety of spin, charge, and orbital states.<sup>1</sup> Extensive investigation of these compounds was first stimulated by the discovery of colossal magnetoresistance (CMR), a large decrease in electrical transport when a magnetic field is applied, which takes place in various compounds near a ferromagnetic transition. Subsequently, the main focus of attention has moved beyond the study of CMR effects in manganites, in particular to the  $x = \frac{1}{2}$  substituted compositions, which in  $\text{La}_{1-x}\text{Ca}_x\text{MnO}_3$  represent the boundary between competing ferromagnetic (FM) and charge-ordered antiferromagnetic (CO-AFM) ground states, a favorable scenario for phase separation (PS) phenomena.<sup>2</sup> Phase separation also occurs in several other systems, and it is most studied in  $(\text{La}_{1-z}\text{Pr}_z)_{0.7}\text{Ca}_{0.3}\text{MnO}_3$  at an intermediate  $z$  doping range,<sup>3</sup> the end members  $z=0$  and  $z=1$  are FM metallic and CO-AFM insulating at low temperatures, respectively. Recent experimental investigations have shown undisputed evidence of the existence of inhomogeneous states and PS in various manganite compounds,<sup>4</sup> a major discovery in the study of strongly correlated electron systems.

In the case of  $\text{La}_{0.5}\text{Ca}_{0.5}\text{MnO}_3$ , the “standard” compound changes on cooling to a FM phase at  $T_C \sim 220$  K and, subsequently, to CO-AFM at  $T_{CO} \sim 150$  K ( $\sim 180$  K upon warming).<sup>5</sup> However, it has been established that this system is better described as magnetically phase segregated over a wide range of temperatures. The nature and properties of this phase-separated state have been the subject of numerous experimental<sup>6–11</sup> and theoretical<sup>2,4</sup> investigations. At low temperatures  $T < T_{CO}$ , FM metallic regions are trapped in a CO-AFM matrix. This is consistent with the sizable bulk magnetization values observed,<sup>6,7</sup> arising from the ferromagnetic component, and with resistivity data, which may show metallic behavior due to the percolation of FM clusters. The fraction of FM phase remaining at low temperatures is

strongly sample dependent. It has been previously demonstrated<sup>7</sup> that the fraction of FM and CO-AFM phases in polycrystalline  $\text{La}_{0.5}\text{Ca}_{0.5}\text{MnO}_3$  can be controlled by appropriate thermal treatments, which produces a continuous change of the relative fraction of the competing FM and CO-AFM phases. The existence of phase separation within the FM phase, i.e., in the intermediate temperature region  $T_{CO} < T < T_C$ , has also been established in various investigations. The occurrence of an incommensurate charge- and orbital-ordered state between  $T_C$  and  $T_{CO}$ , incompatible with ferromagnetic order, was found through transmission electron microscopy.<sup>8,12</sup> Detailed neutron studies<sup>6</sup> reported the appearance below  $T_C$  of a second crystallographic phase structurally different from the FM phase and lacking magnetic order. A consensus has now emerged in the literature regarding the paramagnetic character of this secondary phase,<sup>13–15</sup> although the possible existence of an AFM incommensurate charge-ordered state cannot be ruled out.<sup>8</sup>

Microscopic probes were more successful than magnetic measurements in detecting the intermediate phase-separated state. Indeed, previous magnetization studies appeared to be consistent with the existence of a homogeneous ferromagnetic state at  $T_{CO} < T < T_C$ ,<sup>5,7,16</sup> without any indication of PS. The main reason for the mentioned limitation of the magnetic techniques can be found in the sensitivity of the phase-separated state to the measuring magnetic field,<sup>9,10,17</sup> which can mask the real characteristics of the system in conventional magnetization measurements. In a previous investigation<sup>11</sup> we have shown through transport measurements how the application of a low magnetic field can alter the volume fraction of the competing magnetic phases. When the field is applied while cooling the sample, in a conventional field-cooled-cooling (FCC) experiment, it promotes an enlargement of the FM volume fraction, by preventing the formation of otherwise non-FM regions. On the other hand, if the field is turned on while the measurement is made and turned off while cooling the sample, a procedure called the *turn-on–turn-off* mode, the relative fraction of the existing phases is less disturbed during the cooling process. The mea-

sured magnetoresistance of the compounds differs considerably when comparing data obtained with the FCC and *turn-on–turn-off* modes, since the former enhances the percolation of the FM metallic regions. In fact, it has been theoretically proposed<sup>4,18</sup> and experimentally confirmed<sup>11,15</sup> that the observed colossal magnetoresistance effect in manganites is caused by a field-induced percolative transition of metallic regions in phase-separated systems. Within this scenario, it is possible that a moderate applied field ( $\sim 1$  T) can be high enough to suppress the non-FM phase between  $T_C$  and  $T_{CO}$  in a FCC experiment, giving rise to a magnetic response of the system consistent with a homogeneous state. This is probably the reason for the lack of detection of the intermediate phase-separated state through magnetic measurements.

In this paper we present a detailed magnetization study of phase-separated  $\text{La}_{0.5}\text{Ca}_{0.5}\text{MnO}_3$  manganites, focusing mainly in the intermediate-temperature region  $T_{CO} < T < T_C$ . The samples are a series of polycrystalline compounds, with varying low-temperature volume fraction of FM and CO-AFM phases. We investigated the magnetic response of the system under different measurement procedures, extending the idea related to *turn-on–turn-off*-type measurements to magnetization studies. We found that by changing separately the measuring and cooling field leads to different magnetic responses, providing an important tool to investigate PS effects through magnetization measurements. Using this particular experimental procedure we were able to identify three different regimes in the phase-separated state of  $\text{La}_{0.5}\text{Ca}_{0.5}\text{MnO}_3$  below  $T_C$ , related to the response of the system to the cooling and measuring fields.

## II. EXPERIMENTAL DETAILS

Polycrystalline  $\text{La}_{0.5}\text{Ca}_{0.5}\text{MnO}_3$  was obtained by a standard citrate-nitrate decomposition method. Additional thermal treatments were performed to obtain a batch of samples with different grain sizes. Care was taken to ensure that all samples have the same oxygen stoichiometry, and same Ca doping concentration near 0.5. More details on material preparation and x-ray analysis are given elsewhere.<sup>7</sup> Magnetization measurements were performed with a commercial magnetometer (Quantum Design PPMS) between room temperature and 2 K, with applied fields up to  $H=9$  T. Transport data were obtained with a standard four-point technique. Table I lists some physical parameters of the measured samples, labeled A–E: grain sizes, low-temperature volume fraction of the FM phase, ferromagnetic transition temperature  $T_C$ , and charge-ordered antiferromagnetic transition temperature  $T_{CO}$  measured on cooling. The fraction of FM phase was estimated from  $M$  vs  $H$  measurements at 10 K, as previously described.<sup>7</sup>

## III. RESULTS

In order to characterize the magnetic behavior of the studied compounds, Fig. 1 shows the temperature dependence of the magnetization, measured with  $H=2$  mT for samples A–E. As the temperature is lowered all samples display a

TABLE I. Main characteristics of  $\text{La}_{0.5}\text{Ca}_{0.5}\text{MnO}_3$  samples, labeled A–E. FM (%) is the ferromagnetic phase fraction at low temperatures (Ref. 7),  $T_C$  the ferromagnetic transition temperature, and  $T_{CO}$  the charge-ordered antiferromagnetic transition temperature measured on cooling.  $T_C$  and  $T_{CO}$  were obtained from the maximum inflection of the low-field (2 mT) magnetization data.

Sample	grain size (nm)	FM (%)	$T_C$ (K)	$T_{CO}$ (K)
A	180	84	225	–
B	250	77	219	129
C	450	54	218	137
D	950	15	215	143
E	1300	9	214	147

FM transition at  $T_C$ , followed by a hysteretic first-order transition to a CO-AFM state at  $T_{CO}$  (the latter not visible for sample A). The bulk magnetization measured below  $T_{CO}$  signals the presence of FM domains trapped in the CO-AFM matrix, as previously reported for this material.<sup>6,7</sup> It is clear from the data that the FM volume fraction strongly increases through the series, starting from a compound mostly CO-AFM at low temperatures in sample E and reaching a nearly fully FM material in sample A. The transition temperatures  $T_C$  and  $T_{CO}$ , obtained through the maximum slope of the magnetization data, are listed in Table I. The FM transition decreases from  $T_C \sim 227$  to 214 K for samples A–E, respectively, and the temperature of the CO-AFM transition increases from  $T_{CO} \sim 128$  to 142 K, signaling the stabilization of the CO-AFM phase as the low-temperature FM fraction decreases in the materials. A pronounced irreversibility, i.e.,

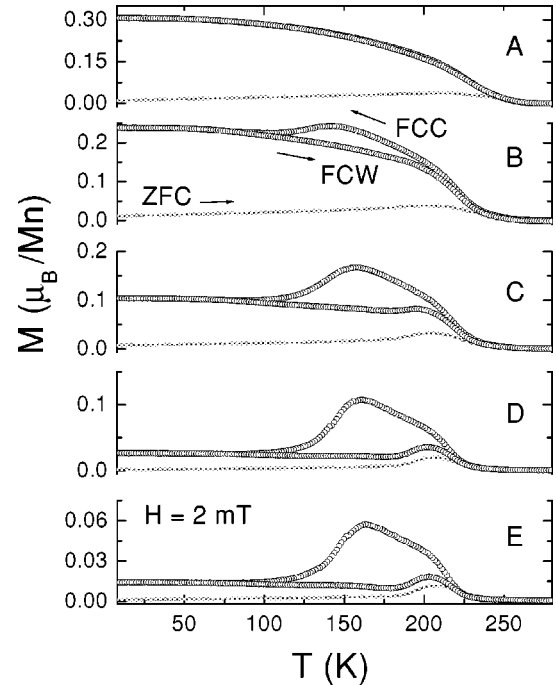


FIG. 1. Magnetization as a function of temperature of  $\text{La}_{0.5}\text{Ca}_{0.5}\text{MnO}_3$  samples, labeled A–E. Results obtained with  $H=2$  mT, with zero-field-cooling (ZFC), field-cooled-cooling (FCC), and field-cooled-warming (FCW) procedures.

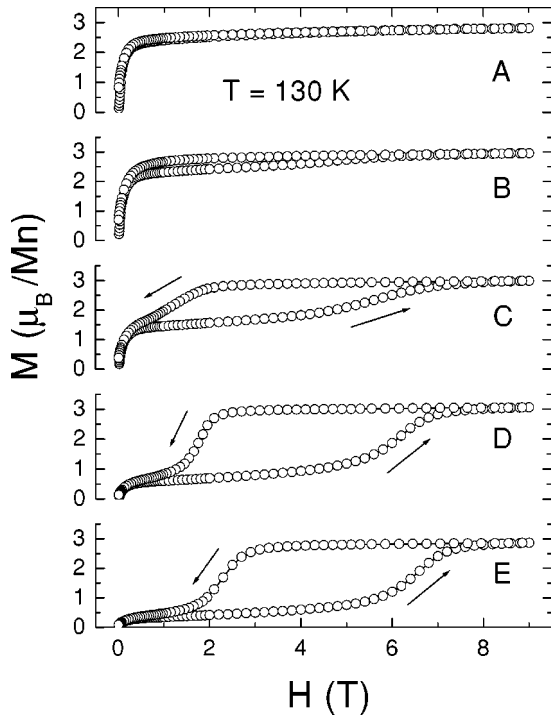


FIG. 2. Magnetization as a function of field of  $\text{La}_{0.5}\text{Ca}_{0.5}\text{MnO}_3$  samples, labeled A–E. Results obtained after zero-field cooling to  $T=130$  K.

the difference between the FCC and zero field-cooled (ZFC) curves, is observed for all samples, as a consequence of the magnetic anisotropy of the compounds. The fractional change  $\xi$  in magnetization, expressed as  $\xi = (M_{FCC} - M_{ZFC}) / M_{FC}$ , has approximately the same value in all samples,  $\xi \approx 0.94 \pm 0.03$  at 10 K. Magnetization measurements at various fields (not shown) reveal little changes in  $\xi$  up to  $H=0.02$  T and a strong decrease above  $H \approx 0.1$  T. This is consistent with the values obtained for the coercive field (a measure of the magnetic anisotropy),  $H_c \approx 0.05$  T at 10 K for all samples. For  $H \gg H_c$ ,  $\xi$  becomes negligible.

The effect of the magnetic field on the coexisting FM and

CO-AFM phases can be readily visualized through measurements of  $M$  vs  $H$ . Figure 2 shows data taken at 130 K, just below the CO transition. It is interesting to observe how the results evolve through the series of samples. For samples D and E, with higher CO-AFM content at low temperatures, the effects due to the FM and AFM phases are clearly separated in the curves. As the field increases it initially aligns the FM moments, followed by a metamagnetic transition of the AFM moments to a field-induced ferromagnetic phase. At this temperature and at the highest field reached, the entire sample is in a FM state. The metamagnetic transition displays large field hysteresis and time relaxation at the fields where  $dM/dH$  is maximum. Samples C and D show a larger initial saturation value of the FM moments and less pronounced hysteresis, related to the increase of the FM fraction and decrease of the CO-AFM fraction in the compounds. Sample A shows data similar to a fully FM sample, consistent with the results of magnetization as a function of temperature (Fig. 1).

We shall now demonstrate that when a magnetic field is applied while cooling the samples it can dynamically change the relative fraction of the magnetic states in this phase-separated material. This phenomenon is investigated by extending to magnetization data the idea of *turn-on–turn-off*-type measurements, where the field is left on at fixed temperatures, while taking a data point, and turned off while cooling the sample. In a more general procedure employed in the present study, the measured magnetization may depend on two different variables  $x$  and  $y$ , where  $x$  is the measuring field and  $y$  the field in which the sample is cooled (both expressed in T). This measuring technique is hereafter called the  $M(x-y)$  mode. Figure 3 displays the results obtained for all samples, comparing the data taken with the FCC and  $M(1-0)$  modes, the latter with a measuring field of 1 T and cooling field zero. The value of 1 T was chosen since it is much above the observed anisotropy field and much below values that would cause a pronounced decrease in  $T_{CO}$  due to melting of the CO state. For sample A, nearly fully FM down to low temperatures, the FCC and  $M(1-0)$  results virtually coincide. As the CO-AFM fraction increases through the se-

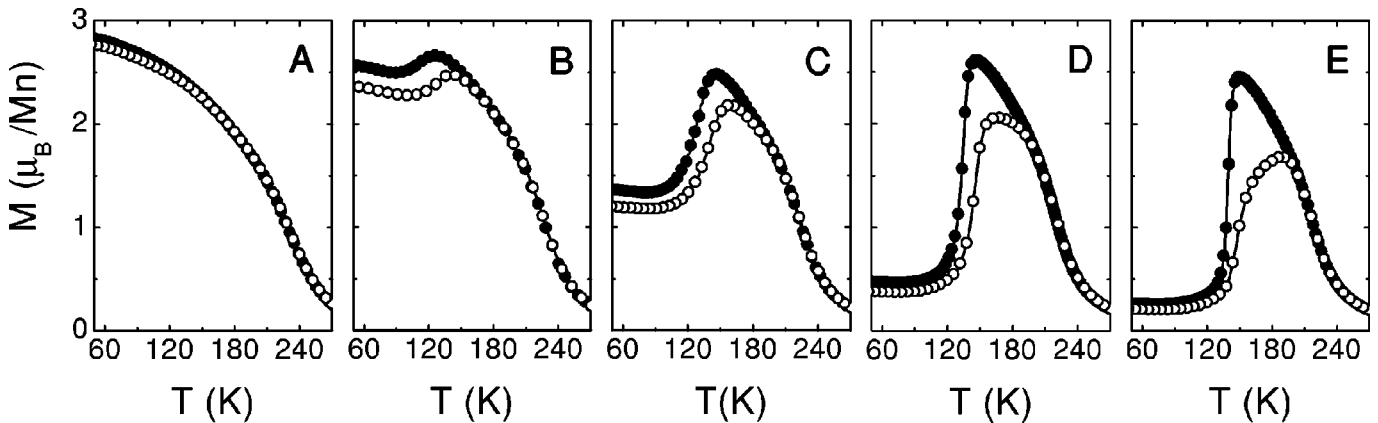


FIG. 3. Magnetization as a function of temperature of  $\text{La}_{0.5}\text{Ca}_{0.5}\text{MnO}_3$  samples, labeled A–E. The curves with solid symbols were measured with a field-cooled-cooling (FCC) mode, with  $H=1$  T. Curves with open symbols obtained with a measuring field  $x=1$  T, and a cooling field  $y=0$ , called the  $M(1-0)$  mode.

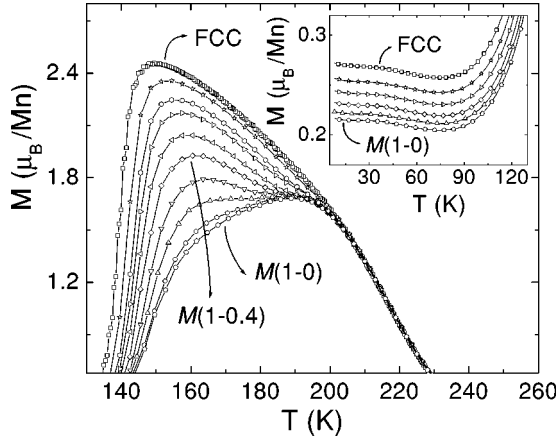


FIG. 4. Magnetization as a function of temperature of  $\text{La}_{0.5}\text{Ca}_{0.5}\text{MnO}_3$ , sample E. Results obtained with a measuring field  $x=1$  T and several values of the cooling field  $y$ , the  $M(1-y)$  mode. The main panel shows an enlarged portion of the data at intermediate temperatures, with (from bottom to top)  $y=0, 0.1, 0.2, 0.3, 0.4, 0.5, 0.6, 0.7,$  and  $0.85$  T. The inset shows the same results at lower temperatures, with  $y=0, 0.2, 0.4, 0.6,$  and  $0.85$  T.

ries the magnetization becomes strongly dependent on whether or not the field is left on while cooling the samples. In samples B and C, below a certain temperature, the  $M(1-0)$  data are shifted with respect to the FCC data. In samples D and E, with higher CO-AFM fraction, it is remarkable to observe huge differences in bulk magnetization when comparing the curves obtained with the two measuring procedures. The temperature where the FCC and  $M(1-0)$  curves separate,  $T_o \approx 200 \pm 2$  K, is nearly unchanged in these two samples and progressively decreases through the series. As discussed below, the change in magnetization depending on the measuring mode is due to the existence of non-FM regions within the FM phase.

Before interpreting these results some points must be verified to ensure the physical meaning of the data. Since the field is being switched on and off continuously in the  $M(x-y)$  mode, one may suspect the samples to be in some kind of magnetic metastable state, where strong relaxation effects would be present. In order to rule out this possibility the  $M(1-0)$  data were repeated, leaving the field on for 30 min and subsequently leaving the field switched off for the same period of time before proceeding to next data point. The observed fractional change in  $M(1-0)$  is always less than 2% at all temperatures. Long-time relaxation data were also taken at selected temperatures, giving a fractional change in  $M(1-0)$  of less than 3% in a period of 4 h. A different test was also made, by varying the temperature interval between data points, from 0.5 to 5 K, with no effect in the  $M(1-0)$  curves. These results clearly establish that the field in which the samples are cooled has an overwhelming effect in the bulk magnetization measured. It is worth noting that the results (not shown) taken while warming the samples, with field-cooled warming and  $M(1-0)$  warming modes (measured after FCC), virtually coincide.

The remainder of this paper will focus on measurements on sample E, with the largest CO-AFM volume fraction at

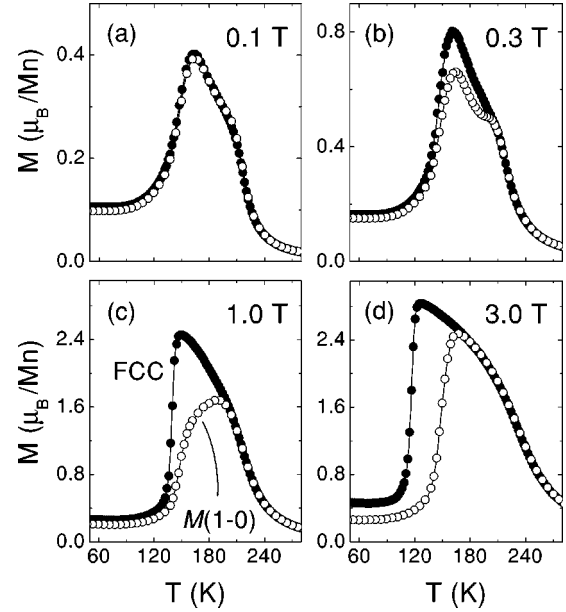


FIG. 5. Magnetization as a function of temperature of  $\text{La}_{0.5}\text{Ca}_{0.5}\text{MnO}_3$ , sample E. The curves with solid symbols were measured with a field-cooled-cooling (FCC) mode, with  $H=0.1$  T (a), 0.3 T (b), 1 T (c), and 3 T (d). Curves with open symbols measured with a cooling field  $y=0$ , the  $M(x-0)$  mode.

low temperatures and where PS effects are more pronounced. Figure 4 shows additional measurements taken in the  $M(x-y)$  mode. The main panel displays the results at intermediate temperatures, while the inset shows an enlarged plot with the low-temperature data. The measuring field was kept constant at  $x=1$  T, and the cooling field  $y$  was varied in order to study its influence on the measured magnetization. The  $M(1-0.06)$  data (not shown for clarity of the figure) are virtually identical to  $M(1-0)$ ; a small difference between  $M(1-0.1)$  and  $M(1-0)$  is observed, and the  $M(x-y)$  curves start to clearly separate from the  $M(1-0)$  data at  $y \geq 0.2$  T. With increasing cooling fields  $y$  the curves gradually evolve towards the data obtained with the FCC mode. With the measuring field kept constant, these results indicate an onset at  $H \approx 0.1$  T above which the cooling field induces changes in the measured magnetization (see Fig. 4). This is consistent with the results shown in Fig. 5(a), where it is shown that with a measuring field of 0.1 T, FCC and  $M(0.1-0)$  results practically coincide. The different panels in Fig. 5 compare data taken with the FCC and  $M(x-0)$  modes. The cooling fields is kept at zero, and the measuring field  $x$  increases from 0.1 to 0.3, 1, and 3 T, respectively. As will be discussed below, the data in the each of the panels of Fig. 5 may be interpreted in a qualitatively different way. The same overall results were obtained on samples B–D, which shows that the cooling field effect is the same regardless of the ratio between the competing FM and CO-AFM phases.

Complementary resistivity measurements are shown in Fig. 6. Three different curves are plotted, corresponding to different experimental procedures: measured without an applied field ( $H=0$ ), measured with  $H=1$  T on the FCC mode, and measured with a field  $x=1$  T while cooled in zero field, the  $R(1-0)$  mode. The inset of Fig. 6 depicts the

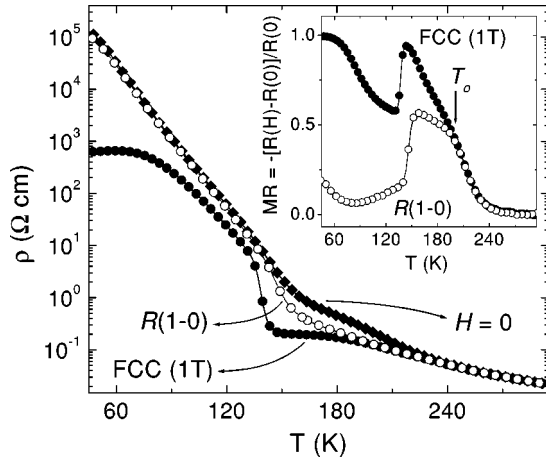


FIG. 6. Resistivity as a function of temperature of  $\text{La}_{0.5}\text{Ca}_{0.5}\text{MnO}_3$ , sample E. Results measured with  $H=0$ , field-cooled cooling with  $H=1$  T and with a measuring field  $x=1$  T and cooling field  $y=0$ , the  $R(1-0)$  mode. The inset depicts the magnetoresistance  $MR = -[R(H)-R(0)]/R(0)$ , calculated for the FCC and  $R(1-0)$  modes; the curves separate at  $T_o$ .

magnetoresistance  $MR = [R(0)-R(H)]/R(0)$ , comparing the results obtained with FCC and  $R(1-0)$  modes. The results clearly show that the large low-temperature MR is solely due to the cooling field, as discussed in more detail in the following section.

#### IV. DISCUSSION

When performing magnetic measurements in phase-separated materials the applied magnetic field can affect the balance between the coexisting phases by increasing the amount of the FM phase, an effect called ferromagnetic fraction enlargement (FFE).<sup>11,15,19</sup> The magnetization response of a phase-separated system involves two field-dependent contributions: the alignment of the magnetic moments of the FM phase and the FFE effect. The applied magnetic field can also lower  $T_{CO}$ , a phenomenon known as melting. It has been argued that PS plays a major role in the melting mechanism, with the competition and coexistence among the FM component and the CO phase causing a drop in the CO transition temperature.<sup>20</sup> Our results (Figs. 3–6) clearly show that the capability of the magnetic field to change the relative fractions of the coexisting phases is strongly dependent on the way in which the field is applied, with the cooling and measuring fields affecting the system in different ways. As previously reported,<sup>11</sup> in a FCC procedure the cooling field induces FFE mainly by inhibiting the formation of the non-FM regions. On the other hand, the measuring field, applied solely at fixed temperatures once the zero-field relative fractions are established, can produce FFE only if it is large enough to transform some fraction of the material from one phase to the other, in a metamagneticlike transition. It must be emphasized that the observed difference in the magnetization curves regarding the way in which the field is applied is a direct consequence of the phase-separated nature of the system. On a nearly homogenous FM sample the magnetization is almost the same in the  $M(x-y)$  and FCC modes, as observed in Fig. 3(a).

The results of Fig. 3 emphasize the fact that regardless of the relative low-temperature fractions of the FM and CO-AFM phases, which is highly dependent on sample preparation, there is an onset temperature  $T_o$  below which the cooling field plays an unbalancing role in favor of the FM state. Measurements displayed in Fig. 4 evidence that above a threshold value of  $H \approx 0.1$  T the FM phase fraction monotonously increases as a function of the applied cooling field. The same threshold field is obtained for the other samples (data not shown). These findings are most likely an intrinsic characteristic of the  $\text{La}_{0.5}\text{Ca}_{0.5}\text{MnO}_3$  system, beyond the particular differences among the samples.

In order to adequately separate the effects of the measuring and cooling fields in the ground state of the system let us call  $\Delta f(x-y)$  the FFE produced when measuring in the  $M(x-y)$  mode and  $\Delta f(x)$  the FFE induced in a FCC procedure. The actual FM phase fraction at a given temperature is proportional to  $(f_0 + \Delta f)$ , where  $f_0$  is the equilibrium fraction of the FM phase at zero field. This notation is useful for a qualitative analysis of Fig. 5, which provides interesting insights into how the magnitude of the applied magnetic field affects the phase-separated state below  $T_C$  by comparing the results measured in the  $M(x-0)$  and FCC modes. Above  $T_o$  the magnetization response is the same in both modes, up to the highest field employed (3 T). The equilibrium state of the sample under the applied magnetic field is the same irrespective of the way in which the magnetic field is applied, so we can conclude that  $\Delta f(x-0) \approx \Delta f(x)$  for  $T > T_o$ .

On cooling below  $T_o$  a different magnetization response arises depending on the measuring mode and on the applied field. While the curves obtained with the extreme fields used (0.1 T and 3 T) show that  $\Delta f(x-0) \approx \Delta f(x)$ , a net distinction between FCC and  $M(x-0)$  modes is observed for 0.3 T and 1 T, indicating that  $\Delta f(x) > \Delta f(x-0)$  for these intermediate fields. In the data measured with  $H=0.3$  T, shown in Fig. 5(b), the difference below  $T_o$  between the FCC and  $M(0.3-0)$  results gives direct evidence of the FFE induced by the cooling field. While the magnetization in the FCC mode continuously increases on cooling across  $T_o$ , the  $M(0.3-0)$  curve shows that a sudden loss of FM phase happens in a small temperature region close below  $T_o$ . On further cooling  $M(0.3-0)$  increases again, indicating that the remaining amount of the FM phase is almost constant until  $T_{CO}$ . Some remarkable differences are found in the  $M(1-0)$  curve [Fig. 5(c)] with respect to  $M(0.3-0)$ . The former also starts to deviate from the FCC curve at  $T_o$ , but continuously decreases on further cooling, contrarily to what happens with  $M(0.3-0)$ . This fact can be attributed to the effect of the measuring field, which in this case is large enough to convert non-FM regions to a FM state. This process is accomplished each time the field is turned on. As the temperature is lowered the capability of the field to produce such transformation decreases. Thus, while  $\Delta f(1\text{ T})$  remains almost constant in the intermediate temperature range,  $\Delta f(1-0)$  decreases as  $T_{CO}$  is approached from above. The capability of even higher measuring magnetic fields to convert the material from non-FM to FM is clearly visualized in Fig. 5(d), where results obtained with the  $M(3-0)$  and FCC

modes coincide above  $T_{CO}$ , indicating that the measuring field is sufficient to induce a nearly complete metamagnetic transition. The above-described scenario is consistent with that proposed by Mahendiran *et al.*,<sup>15</sup> who suggested that the phase coexistence above  $T_{CO}$  is characterized by the existence of CO domains of different sizes and, concomitantly, different critical field values for the local metamagnetic transition.

At  $T_{CO}$  the system changes to a CE-type CO-AFM state.<sup>21</sup> It is well known that below this temperature the phase-separated state is characterized by the coexistence of small FM regions embedded in a CO-AFM matrix. There is negligible FFE induced by the measuring field, whereas the cooling field considerably enhances the low-temperature FM fraction (see inset of Fig. 4). Fast cooling rates also produce the same effect.<sup>22</sup> It is worth noticing that the charge order transition temperature  $T_{CO}$  is lower on the FCC mode as compared to the  $M(x-0)$  mode, because the cooling field enhances the melting of the CO-AFM state. The value of  $T_{CO}$  (obtained through the maximum slope at the decrease of the magnetization) ranges from 146 K at  $H=0.1$  T to 116 K at  $H=3$  T in the FCC mode, but it is almost field independent ( $T_{CO}=146\pm 1$  K) in the  $M(x-0)$  mode. The physical processes occurring in each of the panels of Fig. 5 may be summarized in the following way: 5(a) cooling and measuring fields induce no changes in the magnetic phases; 5(b) cooling field induces FM fraction enlargement; 5(c) cooling field induces FM fraction enlargement and enhanced melting of the CO transition, while the measuring field induces only partial FFE; 5(d) FM fraction enlargement is saturated by both the cooling and the measuring fields above  $T_{CO}$ , and the cooling field also promotes melting of the CO transition.

The resistivity results of Fig. 6 are consistent with this analysis. The onset temperature  $T_o$  below which FCC and *turn-on–turn-off*-type measurements separate is the same in magnetization and resistivity data. Above  $T_o$ , FCC and  $R(1-0)$  resistivity results also coincide. Between  $T_o$  and  $T_{CO}$  the resistivity is lower when cooling in the presence of a magnetic field. It is remarkable to note that below  $T_{CO}$  the magnetoresistance is entirely due to the cooling field. Results with  $H=0$  and with  $H=1$  T applied solely during the measurements practically coincide below  $T_{CO}$ . On the other hand,  $H=1$  T applied while cooling the sample considerably lowers the resistivity. The inset of Fig. 6 shows how the magnetoresistance is enhanced in the FCC mode as compared to the  $R(1-0)$  mode. This confirms that PS effects are responsible for the observed magnetoresistance in this compound. Transport measurements evidence the different ways in which the system reaches the low-temperature CO-AFM state depending on the measuring mode. As the temperature is lowered in the FCC mode a sharp increase of resistivity is observed at  $T_{CO}$ , indicating that CO and AFM states occur simultaneously when cooling under a 1 T field. On the other hand, the zero-field resistivity curve changes nearly smoothly while cooling, suggesting that the fully CO state is reached by a continuous increase of the CO regions below  $T_C$ . The enhanced melting (lower  $T_{CO}$ ) as a result of the cooling field is also observed in the magnetoresistance plot.

The overall behavior observed in  $\text{La}_{0.5}\text{Ca}_{0.5}\text{MnO}_3$  through

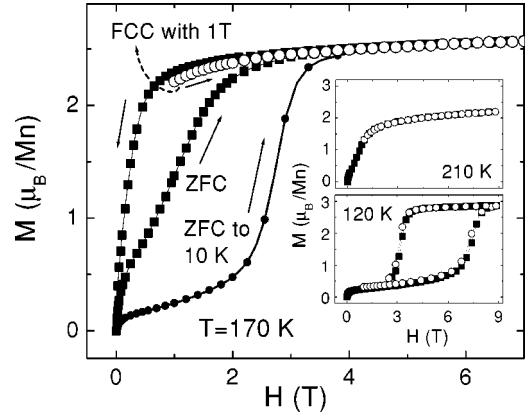


FIG. 7. Magnetization as a function of field of  $\text{La}_{0.5}\text{Ca}_{0.5}\text{MnO}_3$ , sample E. The main panel shows results measured after zero-field cooling (ZFC) to  $T=170$  K (solid squares), after ZFC to  $T=10$  K and subsequently warmed to 170 K (solid circles) and after field-cooled-cooling (FCC) with  $H=1$  T to 170 K (open circles). The insets show data measured after ZFC (solid squares) and FCC (open circles) to  $T=210$  and 120 K.

magnetization measurements, and confirmed by resistivity, shows the existence of well-differentiated regimes in the phase separated state below  $T_C$ . The main characteristics of each regime are clearly visualized in the  $M$  vs  $H$  data showed in Fig. 7. At different temperatures we performed the measurements with a definite experimental procedure: the sample is cooled without an applied field to the target temperature, or alternatively, the sample is cooled with  $H=1$  T to the target temperature. At 210 K (top inset of Fig. 7), in the high-temperature region  $T_o < T < T_C$ , both results coincide. The inhomogeneous FM state that develops at  $T_C$  is characterized by the coexistence of isolated FM clusters embedded in a paramagnetic host.<sup>13,14</sup> With an applied field these clusters can grow freely against the paramagnetic phase, irrespectively of the way in which the field is applied.

The temperature  $T_o$  signals the onset of a different phase-separated state. Following the results of Huang *et al.*,<sup>6</sup> this phase-separated state consists of FM regions coexisting with a structurally different phase. The second phase has different cell parameters than the FM one and is characterized by a major degree of order of the  $d_z^2$  orbital. Traces of PS of a structural nature, with an onset at  $T \approx 200$  K, have also been found in magnetostriction studies.<sup>23</sup> Thus, below  $T_o$ , the FM clusters are structurally confined and cannot grow freely when a magnetic field is applied in the  $M(x-y)$  mode, due to the presence of energy barriers at the phase boundaries. Magnetic relaxation measurements in the intermediate-temperature range also support the above description.<sup>24</sup> These energy barriers increase as the temperature is lowered, and therefore the capability of the measuring field to induce the structural transition from a non-FM to a FM state diminishes. This is responsible for the lower magnetization in the  $M(1-0)$  data of Fig. 5(c). However, the same magnetic field applied in the FCC mode can locally prevent the formation of the secondary phase, giving rise to an enhanced amount of the FM phase with respect to that obtained in the  $M(x-y)$  mode.

The magnetic properties of the intermediate phase-separated state become evident through measurements of  $M$  vs  $H$  at  $T = 170$  K (main panel of Fig. 7). The data recorded after FCC with  $H = 1$  T start from a nearly saturated magnetization value, reflecting that the cooling field almost totally inhibits the formation of the secondary phase. Instead, the results obtained after ZFC to 170 K show a low initial magnetic component, and a smooth metamagneticlike transition, completed at  $H \sim 3-4$  T. An additional curve is displayed, in which the sample is cooled to 10 K and subsequently warmed to the target temperature. In this case the majority phase is the low-temperature AFM-CO phase, which can be transformed to a FM state in a sharp metamagnetic transition, as observed in the figure. Finally, below  $T_{CO}$  most of the material falls into the CO-AFM state, which is robust with respect to the application of moderate magnetic fields, and the relative phase fractions are no longer controlled by the measuring field but only by the cooling field. At 120 K, both ZFC and FCC  $M(H)$  curves (bottom inset of Fig. 7) display the same overall behavior, with an abrupt field-induced CO-AFM to FM metamagnetic transition at  $H \approx 7.4$  T. The data obtained after ZFC and FCC conditions differ only in the magnetization values just above 1 T, due to the FFE effect of the cooling field.

## V. CONCLUSIONS

The present investigation addresses the effects of an applied magnetic field in the magnetic phases of  $\text{La}_{0.5}\text{Ca}_{0.5}\text{MnO}_3$ , one of the prototype compounds for studying PS effects in manganites. The close interplay between the FM fraction and the applied magnetic field is crucial for interpreting the magnetization of this phase-separated system. We have used a particular experimental protocol related to the application of the magnetic field, which reveals the phase-separated nature of the compound, due to the distinguishable effects of the cooling and measuring magnetic fields. The presented magnetization results show the existence of three well-differentiated PS regimes: “soft PS” for  $T_C > T > T_o$ , “intermediate” PS for  $T_o > T > T_{CO}$ , and “hard PS” for  $T < T_{CO}$ . These regimes were identified following the system’s response to an applied magnetic field, and are consistent with neutron scattering results.<sup>6</sup>

The actual existence of a phase-separated state close below  $T_C$  is not directly revealed by our measurements, but was addressed by other authors.<sup>8,12,14,25</sup> In this region the magnetic response of the system is the same in a wide range of magnetic fields, irrespective of the way in which the field is applied. This seems to indicate that the coexisting phases differ in their magnetic properties (paramagneticlike and FM) but do not display energy barriers at the phase boundaries. This fact characterizes the soft PS regime, in which the FM phase can grow almost freely with the application of a magnetic field, whichever mode is employed. The intermediate region has its onset at  $T_o$ , where magnetization curves obtained in the FCC and  $M(x-y)$  modes begin to separate. The different response of the system to the cooling and the measuring fields is consistent with the fact that the phase-

separated state in this temperature range is of a structural nature,<sup>6</sup> with some degree of charge and/or orbital ordering in the secondary phase.<sup>15,26</sup> A moderate applied magnetic field ( $\sim 1$  T) is successful in preventing the formation of the secondary phase in the FCC mode. On the other hand, in the  $M(x-y)$  mode the magnetic field has to induce a structural transition to accomplish the growth of the FM phase against the non-FM one, overcoming the energy barriers at the phase interfaces; therefore, much less FFE is achieved. It is worth noting that the preceding statements are only valid for measuring fields within a definite window, outside which magnetic measurements are unable to reveal the phase-separated nature of the system at this intermediate temperature range. With low magnetic field values ( $H \leq 0.1$  T) even the cooling field does not induce FFE, while at relatively high values ( $H \geq 3$  T) the measuring field alone promotes a complete metamagnetic transition, transforming the system in to a nearly homogeneous FM state.

The hard PS regime which appears below  $T_{CO}$  is the most studied in previous papers. It consists of minority FM regions embedded in an CO-AFM host with CE-type structure, a more robust state with respect to the application of a magnetic field. However, relatively low cooling fields can produce small variations of the FM fraction, which in turn produces huge changes in the resistivity when the FM fraction is near the percolation threshold. The transport data presented provide clear evidence for the percolative nature of the low-field low-temperature colossal magnetoresistance. At temperatures well below  $T_{CO}$ , an applied cooling field is solely responsible for a sizable decrease in electrical transport. On the other hand, there is no appreciable magnetoresistance in measurements with the  $R(x-0)$  mode, since the measuring field cannot produce FFE in the hard PS region. Both transport and magnetization data also show the drastic effect of the cooling field in lowering the CO transition temperature, whereas no reduction in  $T_{CO}$  is observed in the  $M(x-0)$  measurements with fields up to  $\sim 3$  T.

Summarizing, the measured magnetization values in phase-separated manganites depend strongly on the magnetic field applied during the measurements and on the field applied while cooling the sample. We were able to determine through magnetization data the onset at  $T_o$  of the intermediate PS region and established the existence of a critical cooling field above which FFE occurs. The overall results show how *turn-on-turn-off*-type magnetization measurements can be employed to reveal the phase-separated nature of manganite compounds. Needless to say, more powerful tools such as microscopic techniques are required to fully characterize the coexisting phases at the various temperature ranges.

## ACKNOWLEDGMENTS

We thank G. Polla and G. Leyva for sample preparation. This work was partially financed by PRONEX/FINEP/CNPq (Contract No. 41.96.0907.00) and CONICET PEI 125/98. Additional support was given by FAPERJ and by Antorchas, Balseiro, and Vitae Foundations.

- \*Corresponding author. Electronic address: luisghiv@ifufrj.br
- <sup>1</sup>M.B. Salamon and M. Jaime, *Rev. Mod. Phys.* **73**, 583 (2001).
- <sup>2</sup>A. Moreo, S. Yunoki, and E. Dagotto, *Science* **283**, 2034 (1999).
- <sup>3</sup>M. Uehara, S. Mori, C.H. Chen, and S.W. Cheong *Nature (London)* **399**, 560 (1999).
- <sup>4</sup>E. Dagotto, T. Hotta, and A. Moreo, *Phys. Rep.* **344**, 1 (2001).
- <sup>5</sup>P. Schiffer *et al.*, *Phys. Rev. Lett.* **75**, 3336 (1995).
- <sup>6</sup>Q. Huang, J.W. Lynn, R.W. Erwin, A. Santoro, D.C. Dender, V.N. Smolyaninova, K. Ghosh, and R.L. Greene, *Phys. Rev. B* **61**, 8895 (2000).
- <sup>7</sup>P. Levy, F. Parisi, G. Polla, D. Vega, G. Leyva, H. Lanza, R.S. Freitas, and L. Ghivelder, *Phys. Rev. B* **62**, 6437 (2000).
- <sup>8</sup>S. Mori, C.H. Chen, and S-W. Cheong, *Phys. Rev. Lett.* **81**, 3972 (1998).
- <sup>9</sup>G. Allodi, R. De Renzi, M. Solzi, K. Kamenev, G. Balakrishnan, and M.W. Pieper, *Phys. Rev. B* **61**, 5924 (2000).
- <sup>10</sup>Y. Yoshinari, P.C. Hammel, J.D. Thompson, and S-W. Cheong, *Phys. Rev. B* **60**, 9275 (1999).
- <sup>11</sup>F. Parisi, P. Levy, L. Ghivelder, G. Polla, and D. Vega, *Phys. Rev. B* **63**, 144419 (2001).
- <sup>12</sup>C.H. Chen and S-W. Cheong, *Phys. Rev. Lett.* **76**, 4042 (1996).
- <sup>13</sup>A. Simopoulos, G. Kallias, E. Devlin, and M. Pissas, *Phys. Rev. B* **63**, 054403 (2001).
- <sup>14</sup>F. Rivadulla, M. Freita-Alvite, M.A. Lopez-Quintela, L.E. Hueso, D.R. Miguens, P. Sande, and J. Rivas, *J. Appl. Phys.* **91**, 785 (2002).
- <sup>15</sup>R. Mahendiran, A. Maignan, C. Martin, M. Hervieu, and B. Raveau, cond-mat/0107448 (unpublished).
- <sup>16</sup>M. Roy, J.F. Mitchell, A.P. Ramirez, and P. Schiffer, *Phys. Rev. B* **58**, 5185 (1998).
- <sup>17</sup>C. Ritter, R. Mahendiran, M.R. Ibarra, L. Morellon, A. Maignan, B. Raveau, and C.N.R. Rao, *Phys. Rev. B* **61**, R9229 (2000).
- <sup>18</sup>M. Mayr, A. Moreo, J.A. Verges, J. Arispe, A. Feiguin, and E. Dagotto, *Phys. Rev. Lett.* **86**, 135 (2001).
- <sup>19</sup>J. Sacanell, P. Levy, L. Ghivelder, G. Polla, D. Vega and F. Parisi, *Physica B* (to be published).
- <sup>20</sup>Younghun Jo, J.-G. Park, Chang Seop Hong, N.H. Hur, and H.C. Ri, *Phys. Rev. B* **63**, 172413 (2001).
- <sup>21</sup>E.O. Wollan and W.C. Koehler, *Phys. Rep.* **100**, 545 (1955); J.B. Goodenough, *ibid.* **100**, 564 (1955).
- <sup>22</sup>M. Uehara and S-W. Cheong, *Europhys. Lett.* **52**, 674 (2000).
- <sup>23</sup>R. Mahendiran, M.R. Ibarra, A. Maignan, C. Martin, B. Raveau, and A. Hernando, *Solid State Commun.* **111**, 525 (1999).
- <sup>24</sup>J. Lopez, P.N. Lisboa-Filho, W.A.C. Passos, W.A. Ortiz, F.M. Araujo-Moreira, O.F. de Lima, D. Schaniel, and K. Ghosh, *Phys. Rev. B* **63**, 224422 (2001).
- <sup>25</sup>G. Allodi, R. De Renzi, F. Licci, and M.W. Pieper, *Phys. Rev. Lett.* **81**, 4736 (1998).
- <sup>26</sup>Y. Moritomo, *Phys. Rev. B* **60**, 10 374 (1999).